AD-A086 143 BATTELLE COLUMBUS LABS OH F/G 4/2
MULTIWAVELENGTH LIDAR STUDY OF FOG.(U)
MAY 80 B M HERMAN, R M SCHOTLAND DAAG29-76-D-0100
UNCLASSIFIED ERADCOM/ASL-CR-80-0100-1 NL

1 OF 1
AD A086 143

END
DATE FILMED
8-80
DTIC

ASL-CR-80-0100-1

AD
Reports Control Symbol
OSD-1366

MULTIWAVELENGTH LIDAR STUDY OF FOG

LEVEL II

MAY 1980

By

B. M. Herman
R. M. Schotland

The University of Arizona
Tucson, Arizona 85721

Under Contract: DAAG29-76-D-0100

Contract Monitor: Jagir Randhawa

Approved for public release; distribution unlimited

US Army Electronics Research and Development Command
ATMOSPHERIC SCIENCES LABORATORY
White Sands Missile Range, NM 88002

NOTICES

Disclaimers

The findings in this report are not to be construed as an official Department of the Army position, unless so designated by other authorized documents.

The citation of trade names and names of manufacturers in this report is not to be construed as official Government indorsement or approval of commercial products or services referenced herein.

Disposition

Destroy this report when it is no longer needed. Do not return it to the originator.

SECURITY CLASSIFICATION OF THIS PAGE *(When Data Entered)*

REPORT DOCUMENTATION PAGE

READ INSTRUCTIONS BEFORE COMPLETING FORM

1. REPORT NUMBER: ASL-CR-80-0100-1	2. GOVT ACCESSION NO.: AD-A086 143
3. RECIPIENT'S CATALOG NUMBER:	
4. TITLE *(and Subtitle)*: MULTIWAVELENGTH LIDAR STUDY OF FOG.	5. TYPE OF REPORT & PERIOD COVERED: R&D Technical Report.
	6. PERFORMING ORG. REPORT NUMBER:
7. AUTHOR(s): B. M. Herman; R. M. Schotland	8. CONTRACT OR GRANT NUMBER(s): DAAG29-76-D-0100
9. PERFORMING ORGANIZATION NAME AND ADDRESS: The University of Arizona, Tucson, Arizona 85721	10. PROGRAM ELEMENT, PROJECT, TASK AREA & WORK UNIT NUMBERS: 1L162111AH71-23
11. CONTROLLING OFFICE NAME AND ADDRESS: US Army Electronics Research and Development Command, Adelphi, MD 20783	12. REPORT DATE: May 1980
	13. NUMBER OF PAGES: 36
14. MONITORING AGENCY NAME & ADDRESS *(if different from Controlling Office)*: Atmospheric Sciences Laboratory, White Sands Missile Range, NM 88002	15. SECURITY CLASS. *(of this report)*: UNCLASSIFIED
	15a. DECLASSIFICATION/DOWNGRADING SCHEDULE:

16. DISTRIBUTION STATEMENT *(of this Report)*

Approved for public release; distribution unlimited.

17. DISTRIBUTION STATEMENT *(of the abstract entered in Block 20, if different from Report)*

18. SUPPLEMENTARY NOTES

Jagir Randhawa, ASL, Monitor

19. KEY WORDS *(Continue on reverse side if necessary and identify by block number)*

Fog
Multiwavelength
Lidar liquid water content
Extinction and backscatter coefficient

20. ABSTRACT *(Continue on reverse side if necessary and identify by block number)*

A study has been conducted to define quantitatively the range and accuracy of multispectral lidar techniques for remotely sensing the visibility and liquid water content of various types of fogs. The results indicate that the penetration of the lidar pulse into the fog is limited to a few hundred meters due to the severe attenuation of the pulse by the fog. Methods to obtain extinction, backscatter and total liquid water content are also discussed.

DD FORM 1 JAN 73 1473 EDITION OF 1 NOV 65 IS OBSOLETE

SECURITY CLASSIFICATION OF THIS PAGE *(When Data Entered)*

407080

CONTENTS

1. Purpose of Study

The main objective of this study, as originally set forth in work statement 79-277, is to define quantitatively the range and accuracy of multispectral lidar techniques for remotely sensing the visibility, size distribution, concentration, and liquid water content of various types of fogs. As outlined in the above work statement, the study was to include three lidar wavelengths (0.53 μm, 1.06 μm, and 10.6 μm). Radiation and advection fogs with visibilities of 30 — 1000 meters were to be investigated to ascertain, first, from a single wavelength, how well the above parameters could be determined, and second, using information from three wavelengths, whether the errors in the determinations could be reduced. Finally, the maximum useful ranges for 1.06 μm and 10.6 μm wavelengths were to be found for the given range of visibilities, and the importance of multiple scattering was to be determined.

The original work order was subsequently modified (personal communication with Dr. J. S. Randhawa), and the study was narrowed down to the following objectives:

a. Four lidar wavelengths, representing currently available systems within the wavelength region of interest, were to be studied. The wavelengths are 0.53 μm, 1.06 μm, 3.8 μm, and 10.6 μm.

b. Lidar performances and signal-to-noise (S/N) ratios are to be ascertained for representative systems at these wavelengths.

c. Maximum useful ranges at the 4 wavelengths were to be determined.

d. Methods to obtain extinction, back-scatter and total liquid water content were to be investigated.

It was agreed that the question of obtaining size distributions and the effects of multiple scattering would not be considered here, due to the complexity of these problems and the time restrictions on the present work.

2. Discussion of Fog Models

In order to perform the required calculations for this study, it is necessary to model the distribution of droplet sizes composing the fogs, as the optical parameters (*i.e.*, extinction, backscatter, optical depth) will depend upon the chosen distributions. While many fog distributions are described in the literature, it was decided that those given by Pinnick *et al.* (1978) were most relevant and convenient for the purposes of this study. Pinnick *et al.* have conveniently fit observed size distributions to a superposition of two log-normal distribution functions (see Fig. 1) and have listed the values of the appropriate parameters for each. The advantage of the Pinnick distributions is that the analytic form renders them easily amenable to computer calculations. Furthermore, by varying the parameters of the log-normal functions, variations of the initial distributions may readily be generated with considerably less computer effort.

The log-normal distribution function is given by

$$\frac{dn(r)}{dr} = \frac{1}{(2\pi)^{\frac{1}{2}} r\sigma} \exp\left[-(\ell n\, r - \ell n\, \bar{r})^2/2\sigma^2\right] \qquad (1)$$

Here, $n(r)$ is the number of particles per unit volume of radius r, $\bar{r}$ is the mean radius, and σ is the natural log of the standard deviation of r.

The first distribution given by Pinnick *et al.*, which we here refer to as distribution A or dist. A, is a superposition of two log-normal functions with parameters $\bar{r}$ = 0.3 μm, σ = 1.87, and total liquid water content (LWC) = 1.65×10^3 μg/m^3, and $\bar{r}$ = 4.4 μm, σ = 1.47, and LWC = 1.60×10^5 μg/m^3. The second distribution, distribution B or dist. B, has parameters $\bar{r}$ = 0.6 μm, σ = 2.5, and LWC = 7.52×10^4 μg/m^3 and $\bar{r}$ = 5.0 μm, σ = 1.65, and LWC = 4.37×10^3 μg/m^3. Plots of distributions A and B are shown in Fig. 1.

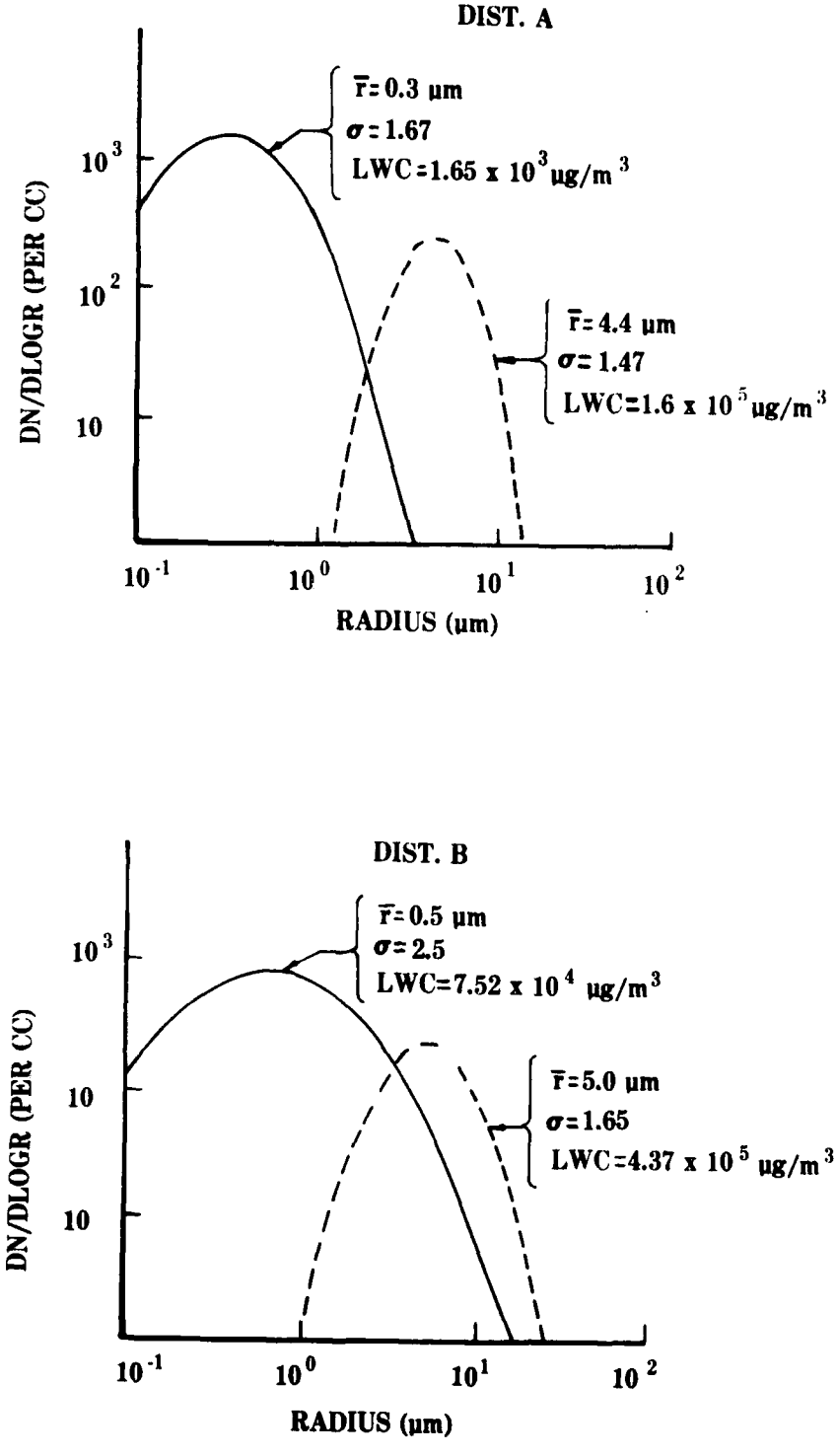

Figure 1. Size distributions (from Pinnick et al 1978) used for the calculations presented in this report. (See text for a discussion of the modifications to the above two distributions that were also employed.)

Besides the standard distributions A and B as listed above, new distributions were generated as follows. The liquid water content of the two individual log-normal functions making up distribution A are in the ratio of about 97:1, while those making up distribution B are in the ratio 5.6:1. By keeping the same the individual normalized log-normal functions which make up each distribution, but varying the ratio of the LWC's, a wide range of new size-distribution functions may be generated. This method has the advantage of not requiring repeated calculations for each new distribution. Once the optical properties, such as volume extinction or backscattering coefficient, have been determined for each individual log-normal function in each distribution, these properties need be simply multiplied by the proper constants to provide the required ratios of the LWC's. Liquid water content ratios of the two log-normal functions making up each distribution were varied from 1000:1 to 0.1:1. A few of the resulting size distribution functions are shown in Figs. 2 through 7.

3. Computation of Optical Properties

Use of the lidar equation requires knowledge of the volume extinction coefficient, Q_{TV}, and the volume backscatter coefficient, β, in order to perform calculations of the returned signal and the S/N ratios to be expected. The calculations of Q_{TV} and β were performed as follows.

Calculations of the backscatter cross section, $\beta(r)$, and extinction cross section, $Q_T(r)$, for a particle of radius r were made, using the standard Mie equations and the appropriate complex indices of refraction. These are related to the volume coefficients through the relationships

$$Q_{TV} = \int_0^\infty Q_T(r) \frac{dn(r)}{dr} dr \qquad (2a)$$

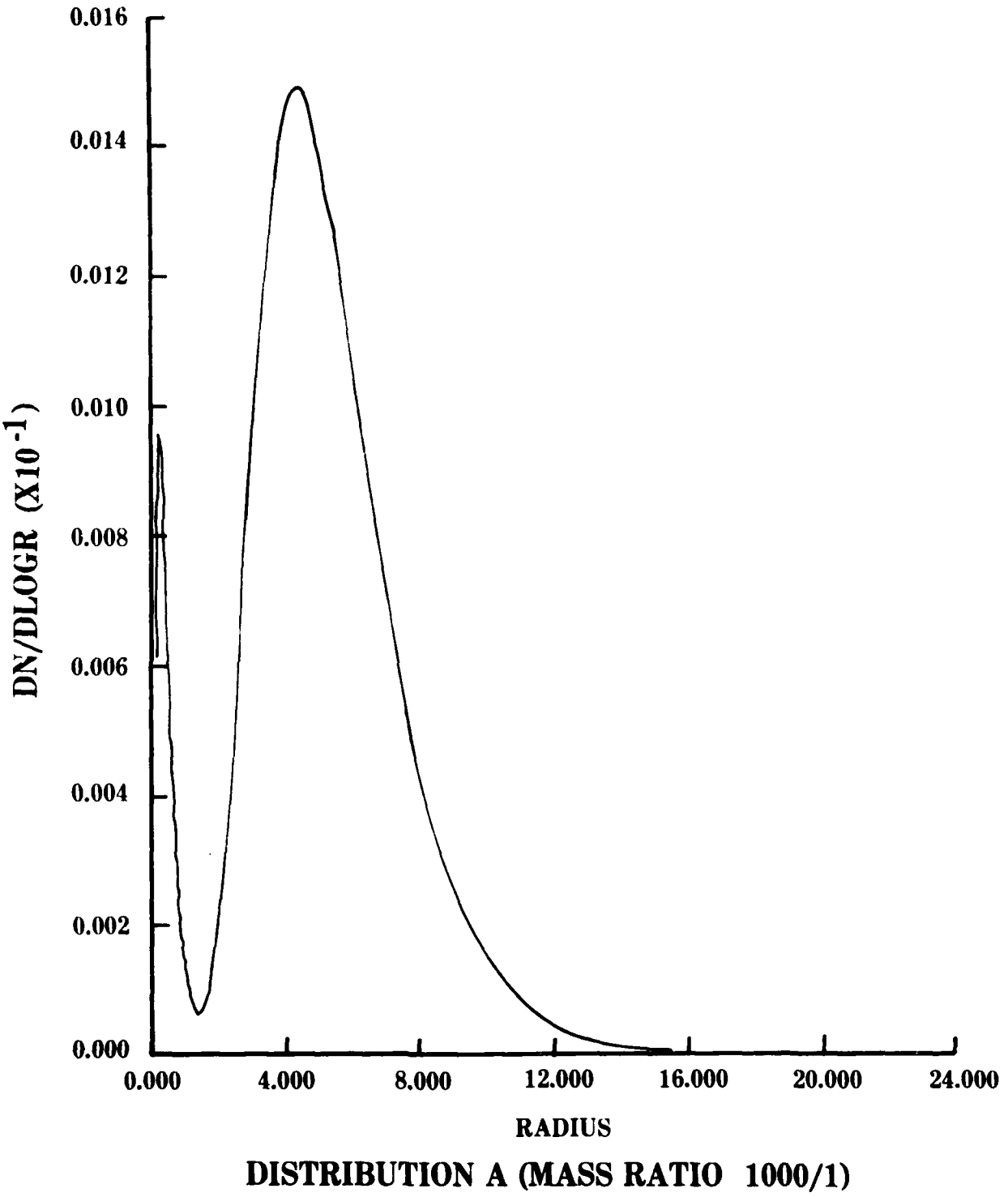

Figure 2. Log-normal distribution function as calculated for various sizes (for Distribution A, mass ratio = 1000/1).

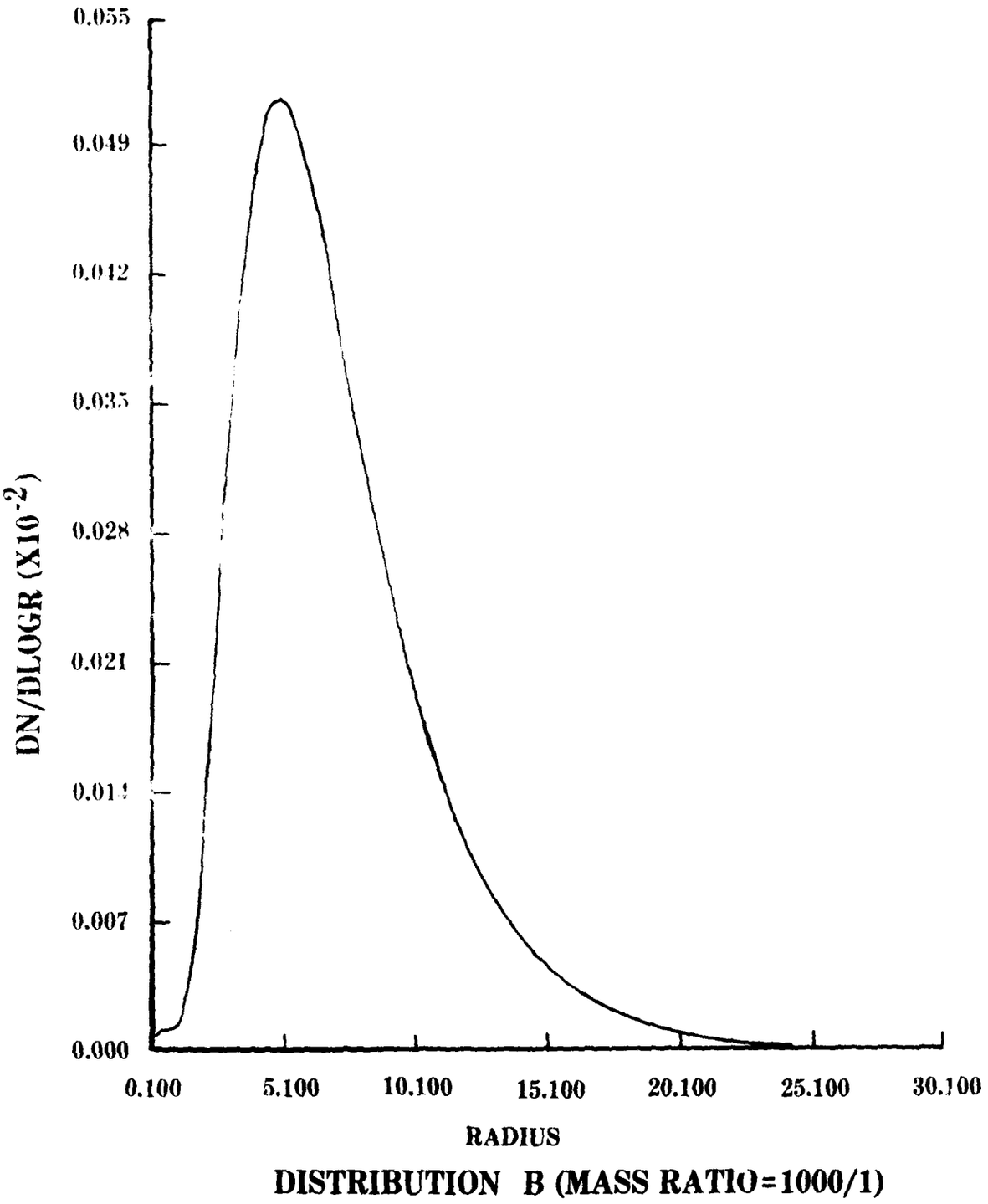

Figure 3. Same as in figure 2 (Distribution B).

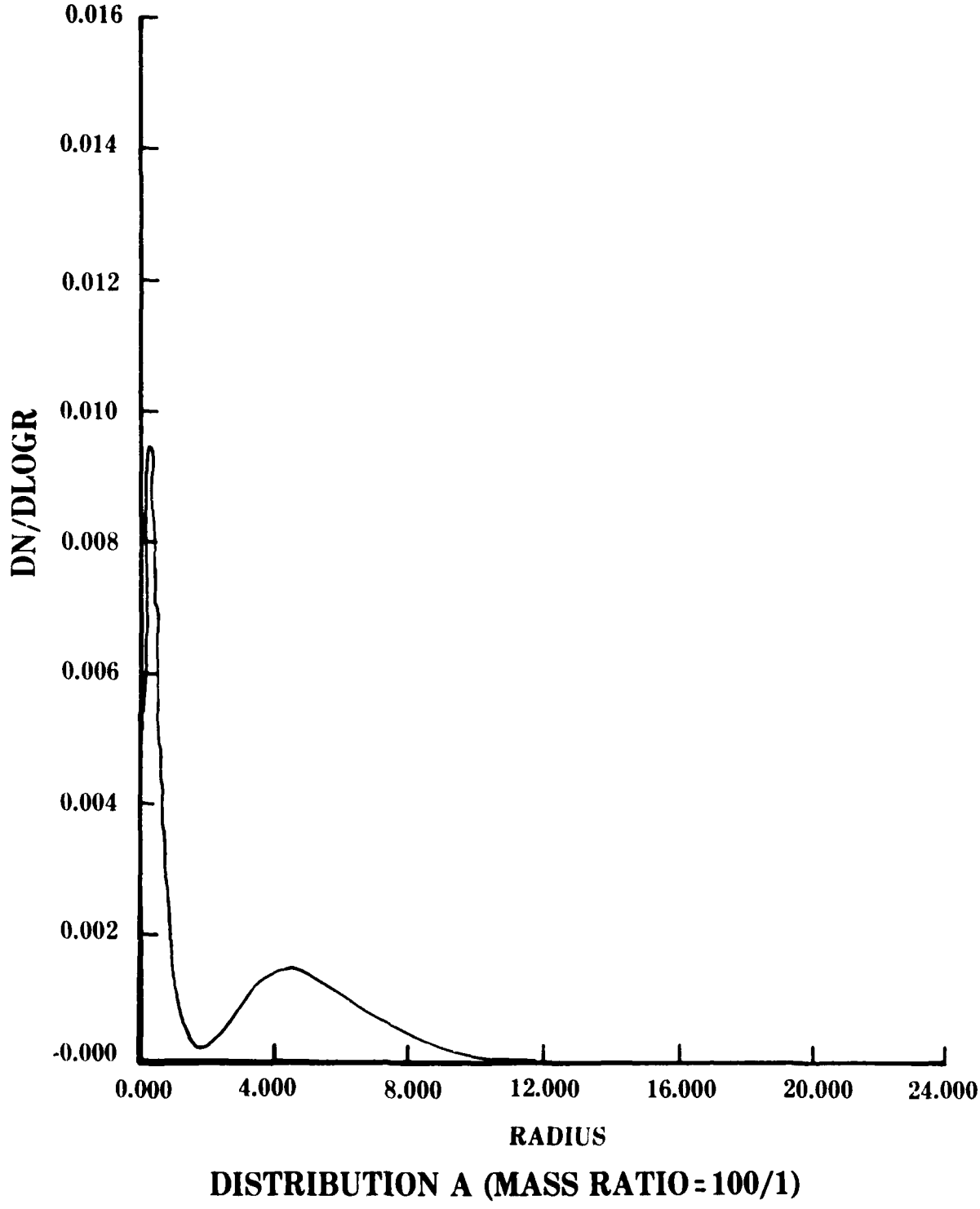

Figure 4. Log-normal distribution function as calculated for various sizes (for Distribution A, mass ratio = 100/1).

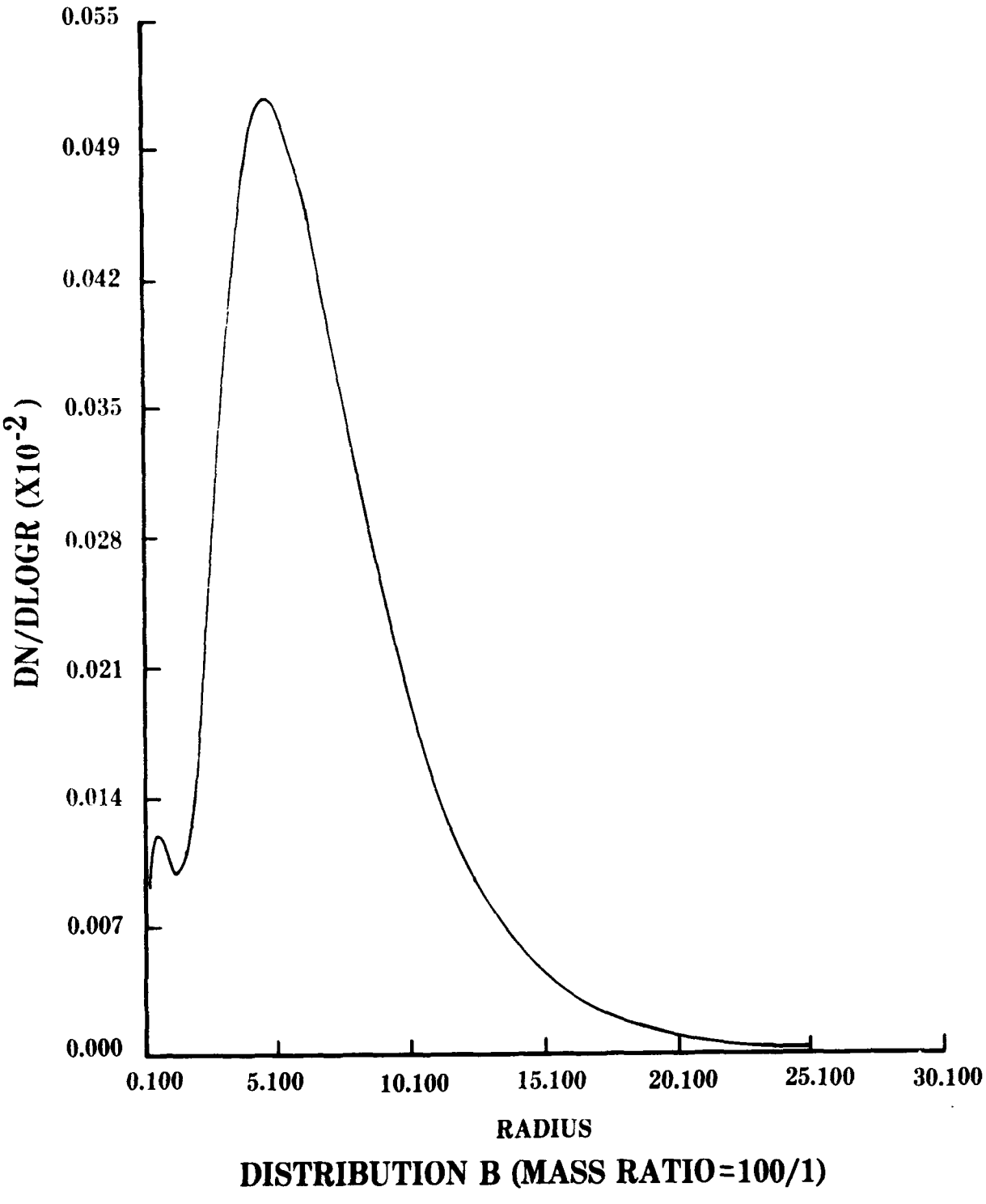

Figure 5. Same as in figure 4 (Distribution B).

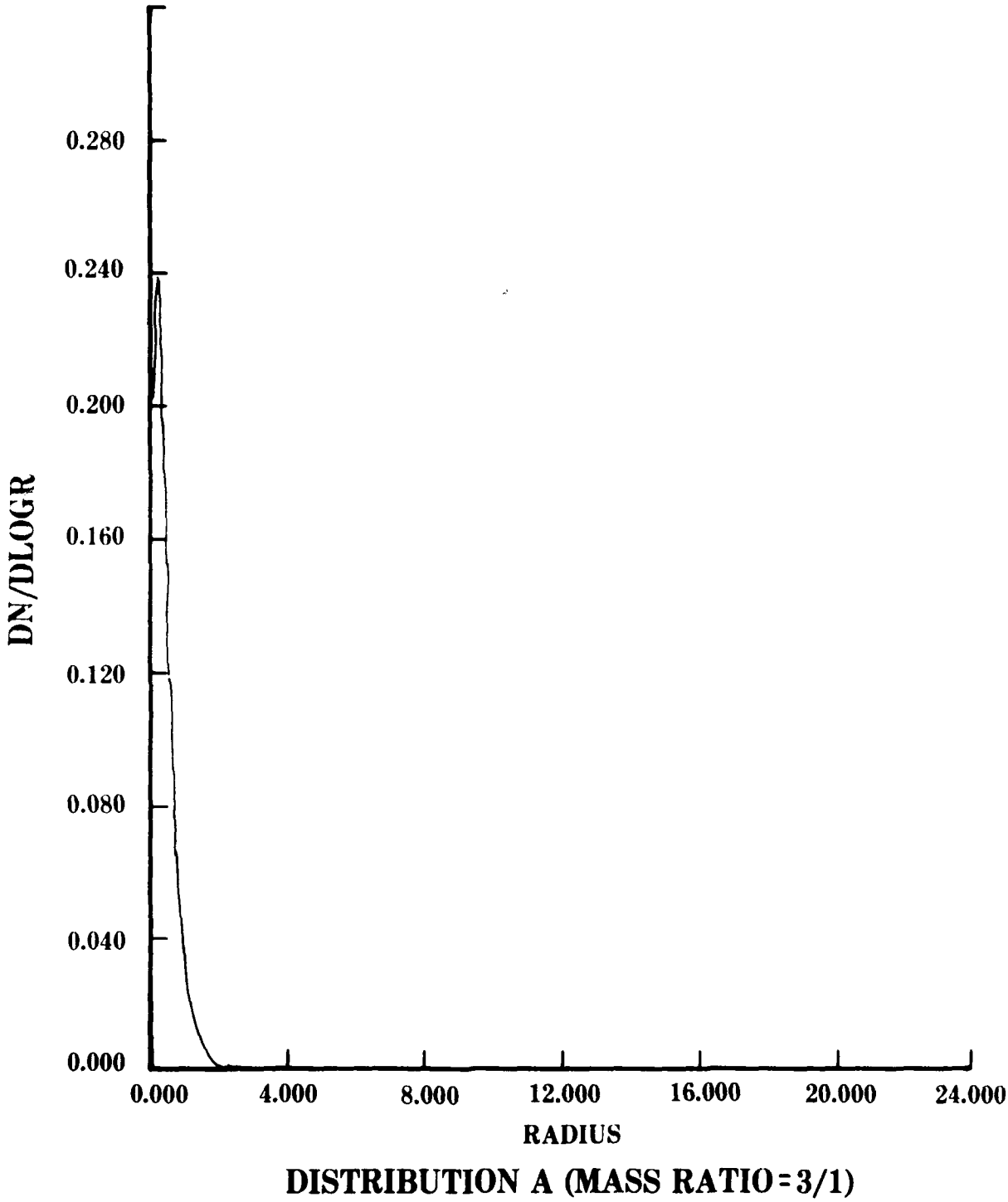

Figure 6. Log-normal distribution function as calculated for various sizes (for Distribution A, mass ratio = 3/1).

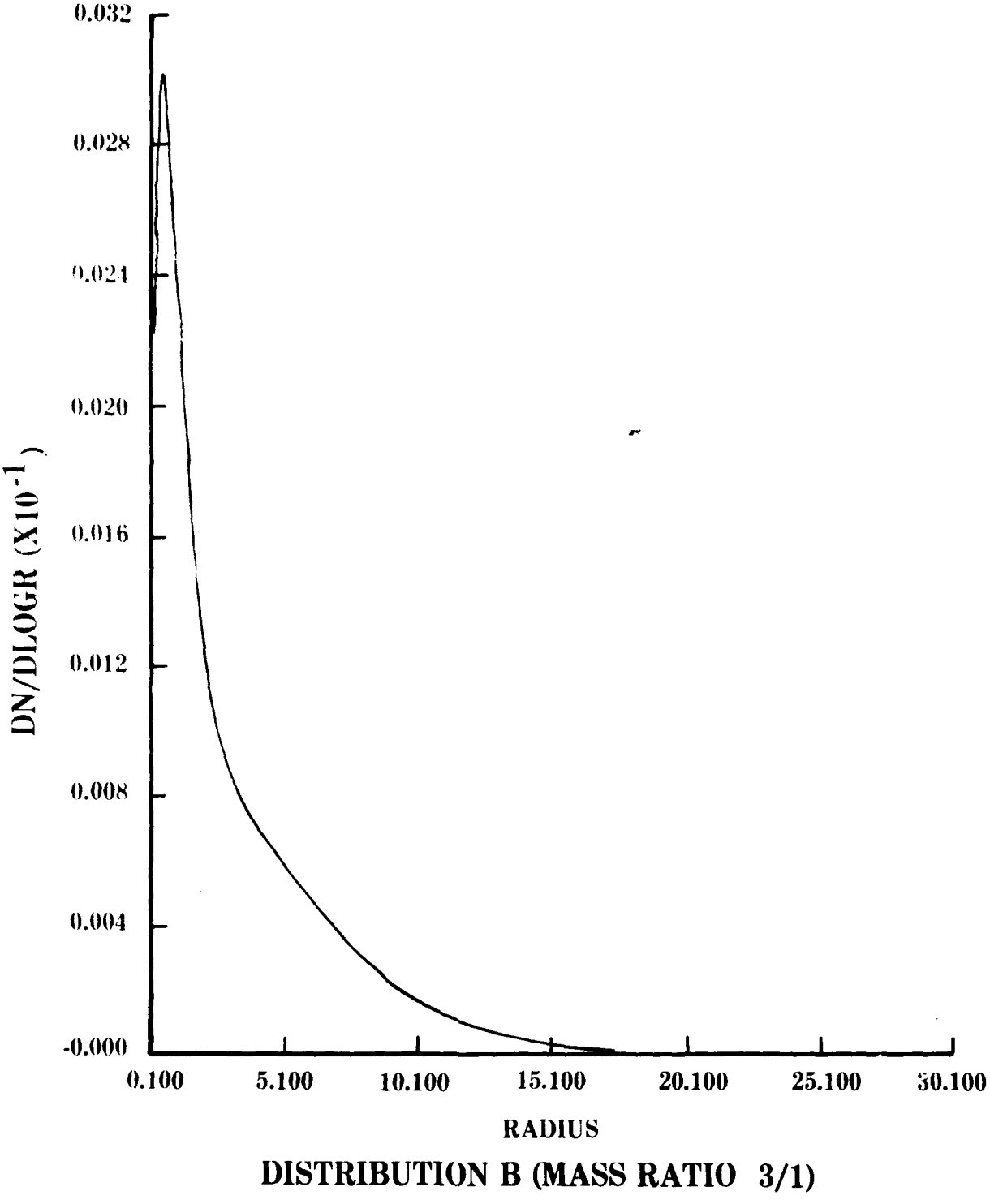

Figure 7. Same as in figure 6 (Distribution B).

and

$$\beta = \int_0^\infty \beta(r) \frac{dn(r)}{dr} dr , \qquad (2b)$$

where $[dn(r)]/dr$ is one of the Pinnick distributions or its modifications, as discussed in section 2. In practice, the integrations were carried out numerically for each of the two log-normal distributions in dist. A and dist. B. Then the total LWC for each log-normal distribution was computed from the equation

$$LWC = \int_0^\infty \rho \; 4/3 \; \pi r^3 \frac{dn(r)}{dr} dr$$

where ρ is the density of liquid water (=1.0). Then the individual log-normal distributions for the two fog types (dist. A and dist. B) were multiplied by the proper constants to bring the individual LWC's into the required ratios. These constants were then used to combine the values of Q_{TV} and β for the individual log-normals, to give the required values for dist. A and dist. B. Once the log-normals were combined, they were then renormalized so that dist. A and dist. B each represented a total liquid water content of 1 gm/m^3 for the modified Pinnick distributions. The liquid water content for the original Pinnick distributions was set as given by Pinnick *et al.*, *i.e.*, 0.161 gm/m^3 for dist. A and 0.512 gm/m^3 for dist. B. Thus the modified Pinnick distributions represent approximately 2 - 5 times the LWC as originally measured by Pinnick. However, these modified distributions can be used for any desired LWC by simply multiplying the present results by the proper renormalizing constant. The calculations of S/N ratios presented in section 3 used the original LWC as given by Pinnick *et al.*

Figures 8 and 9 show Q_{TV} for a fixed LWC = 1 gm/m^3, as a function of the various modified Pinnick distributions A and B for each of the four

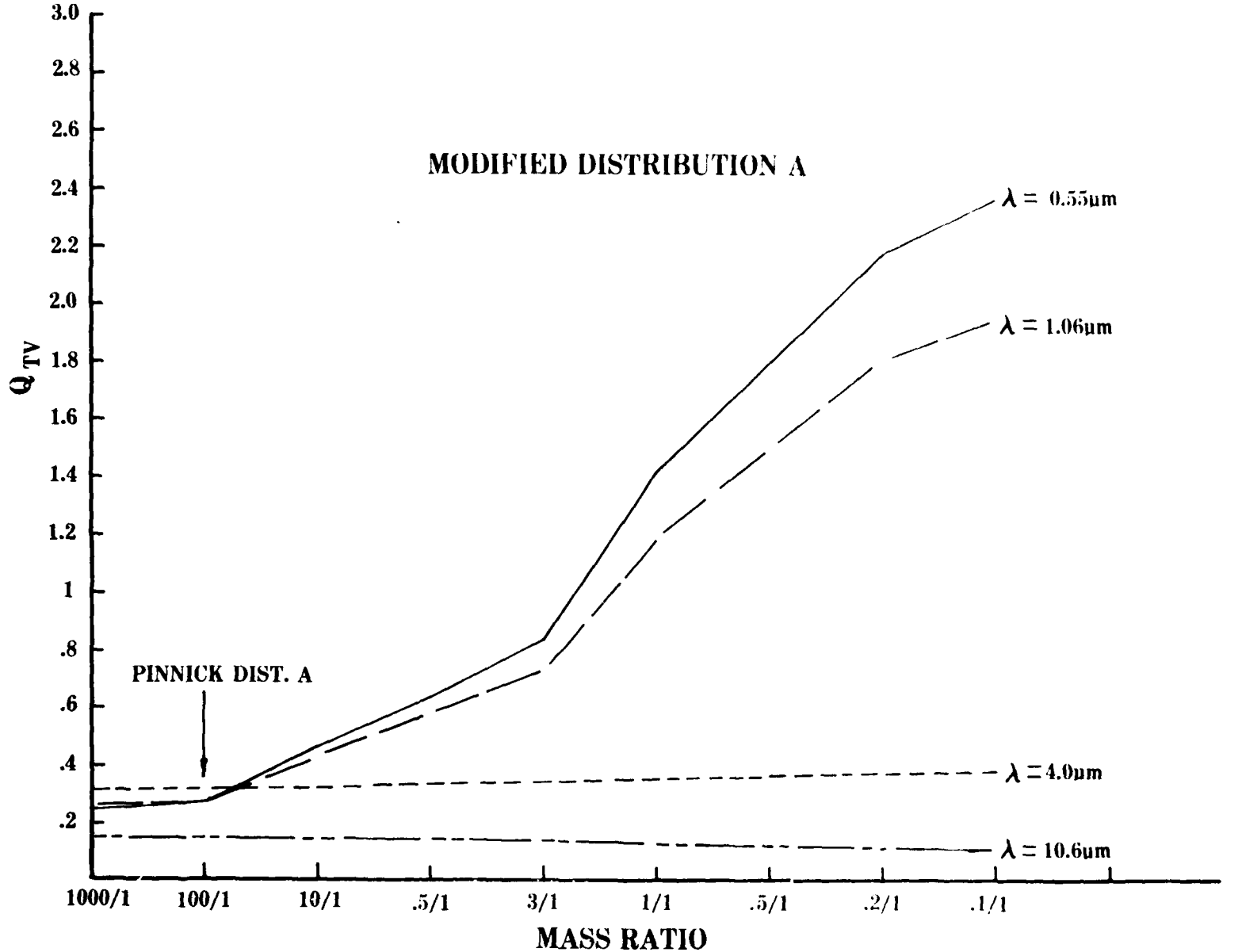

Figure 8. Volume extinction coefficient plotted against modified Distribution A for each of four wavelengths

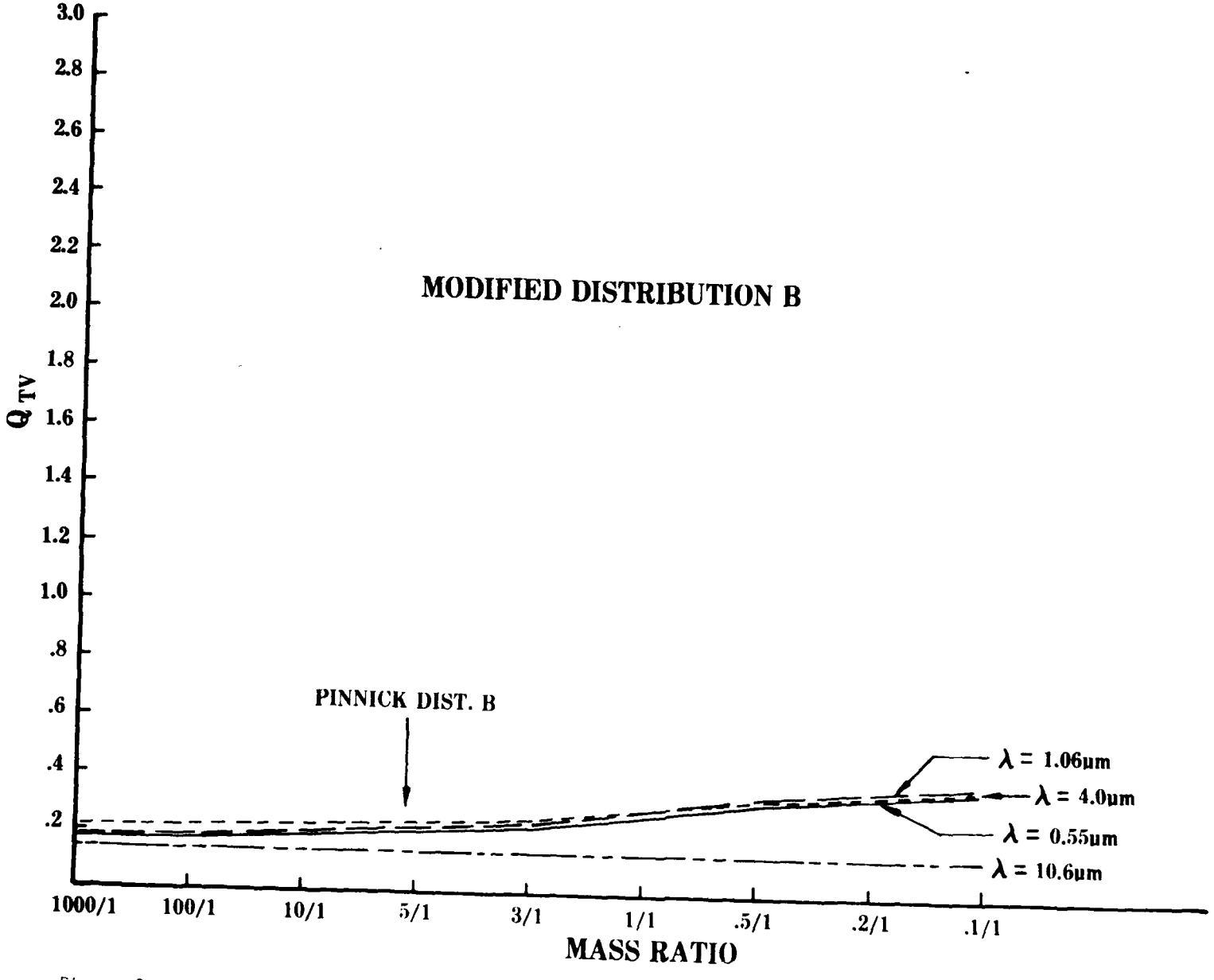

Figure 9. Same as in figure 8 for modified Distribution B.

selected wavelengths. The abscissa in these figures represents the mass ratios of the two log-normal functions making up each distribution.

These figures are interesting in that they show clearly the importance of the drop-size spectrum in determining the resulting optical properties of the fog, particularly for the modifications of distribution A. Here, at the two shorter wavelengths (λ = 0.55 μm and λ = 1.06 μm), the extinction changes by about one order of magnitude over the range of modified distributions considered. It is important to remember that all distributions in these figures have been normalized to the same LWC, so the effects are due solely to the different drop-size spectra. For distribution B, the changes are less dramatic, being approximately a factor of 2 over the complete set of size distributions at the three shorter wavelengths. Of perhaps more significance is the fact that, at 10.6 μm, and to some extent at 4.0 μm, for all modifications of both dist. A and dist. B, the volume extinction is nearly constant. This suggests the possibility of using the determination of Q_{TV} as a direct measure of the LWC of the fog. This is discussed in section 5.

4. Lidar Techniques

a. Lidar Equation

The lidar equation for a pulsed coaxial system can be written as

$$P_r = A \frac{cJ_\lambda}{2R^2} \beta \exp - 2 \int_0^R Q_{TV}\, dz \qquad (3)$$

where P_r = the radiation backscattered to the lidar receiver,

A = the area of the receiver,

J_λ = the energy in the transmitted laser pulse,

R = the range to the scattering pulse,

β = the differential backscattering cross section per unit volume of scattering medium,

and Q_{TV} = the medium extinction cross section per unit scattering volume.

Three assumptions have been made in the development of this equation. The first of these is that the scattering process is the result of single scattering; multiple scattering is ignored. The second assumption is that molecular scattering can be ignored when compared to the fog droplet scatter. This follows, since the differential molecular volume backscatter cross section at sea level is approximately 10^{-8} m^{-1}/sr compared to 10^{-3} m^{-1}/sr for fog. These values are for a wavelength of 0.55 μ, which would magnify the molecular scattering contribution when compared with values at longer wavelengths.

The third assumption is that the attenuation of the laser pulse is brought about solely through fog droplet scattering and absorption losses. The laser wavelengths have been chosen such that molecular absorption can be ignored. Molecular scattering can be neglected using arguments similar to those used in discussing the volume scattering cross sections.

b. Lidar Parameters

Four lidar systems have been chosen for analysis; these lidars operate in spectral regions of interest to the sponsoring agency. The parameters listed below for the lidars represent available components near the state of the art. Wavelengths are listed in microns, and energy is measured in joules.

TABLE I

λ(μ)	Energy (J)	System Transmittance	Filter Width (μ)	Detector
.53	.2	.6	10^{-3}	S-20
1.06	1	.4	10^{-3}	Avalanche Diode
3.8	1	.6	2×10^{-2}	InSb
10.6	10	.8	2×10^{-2}	HgCdTe

In each case, the receiver aperture was taken to be 0.5 m in diameter, the receiver field of view to be 10^{-5} sr, and the signal processing bandwidth to be 10^{7} Hz.

c. Lidar Performance

Signal-to-noise (S/N) calculations have been performed for the lidar system described above. It was assumed in these calculations that the lidars were immersed in a ground fog of the type described in Fig. 1, taken from the paper by Pinnick *et al.* (1978). In order to consider a wider range of fog conditions, the analysis was also performed for five fogs having the same size distribution but with liquid water contents ranging from a factor of two larger than the original distribution to a factor of 1/8 the original fog.

The differential volume backscattering cross sections, β ($m^{-1}sr^{-1}$), and the extinction coefficients, Q_{TV} (m^{-1}) for the basic distributions are as follows.

TABLE II

(See Figure 1 for description of distributions A and B)

Wavelength	Q_{TV}		β	
	(Dist. A)	(Dist. B)	(Dist. A)	(Dist. B)
.53	.443E-01	.104E+00	.206E-02	.526E-02
1.06	.449E-01	.108E+00	.200E-02	.499E-02
3.8	.519E-01	.118E+00	.878E-03	.244E-02
10.60	.237E-01	.695E-01	.219E-04	.497E-04

In order to determine the S/N ratio, it was necessary to make an assumption as to the levels of the background radiation. These values were determined, in the case of those lidars working at wavelengths 4 microns and less,

by scattering the appropriate solar irradiance isotropically. These values agree within a factor of 2 of those suggested in Wolfe and Zissis (1978). It was assumed for the 10.6 micron system that the background level originated from the fog acting as a black body.

The signal level as a function of range was computed using Eq. (3) and the system parameters listed in Tables I and II for each of the two basic size distributions. The system noise was determined, according to the type detector used in each system, from typical manufacturer specifications. The system noise is somewhat range-dependent, since it depends upon both the constant intrinsic detector noise and background noise, as well as the time-varying signal shot noise. The detection process was considered to be incoherent, and all the results are valid for single pulses (*i.e.*, no S/N enhancement through averaging).

The results of these calculations are presented in Figs. 10 through 17.

5. Data Evaluation

a. Determination of Optical Properties of Fog

Reference to the curves of signal-to-noise ratio as a function of fog penetration indicates that useful lidar signals can be measured only over distances of the order of a few hundred meters. It should also be recognized that the fog droplet concentration as well as size distribution will fluctuate, both with time and with position within the fog. Consequently, it seems reasonable that effective values of both β and Q_{TV} be derived from the lidar measurements which represent both temporal and spatial averages of these cross sections.

Equation (3) can be written explicitly in terms of the spatial and temporal fluctuations in β and Q_{TV} as follows.

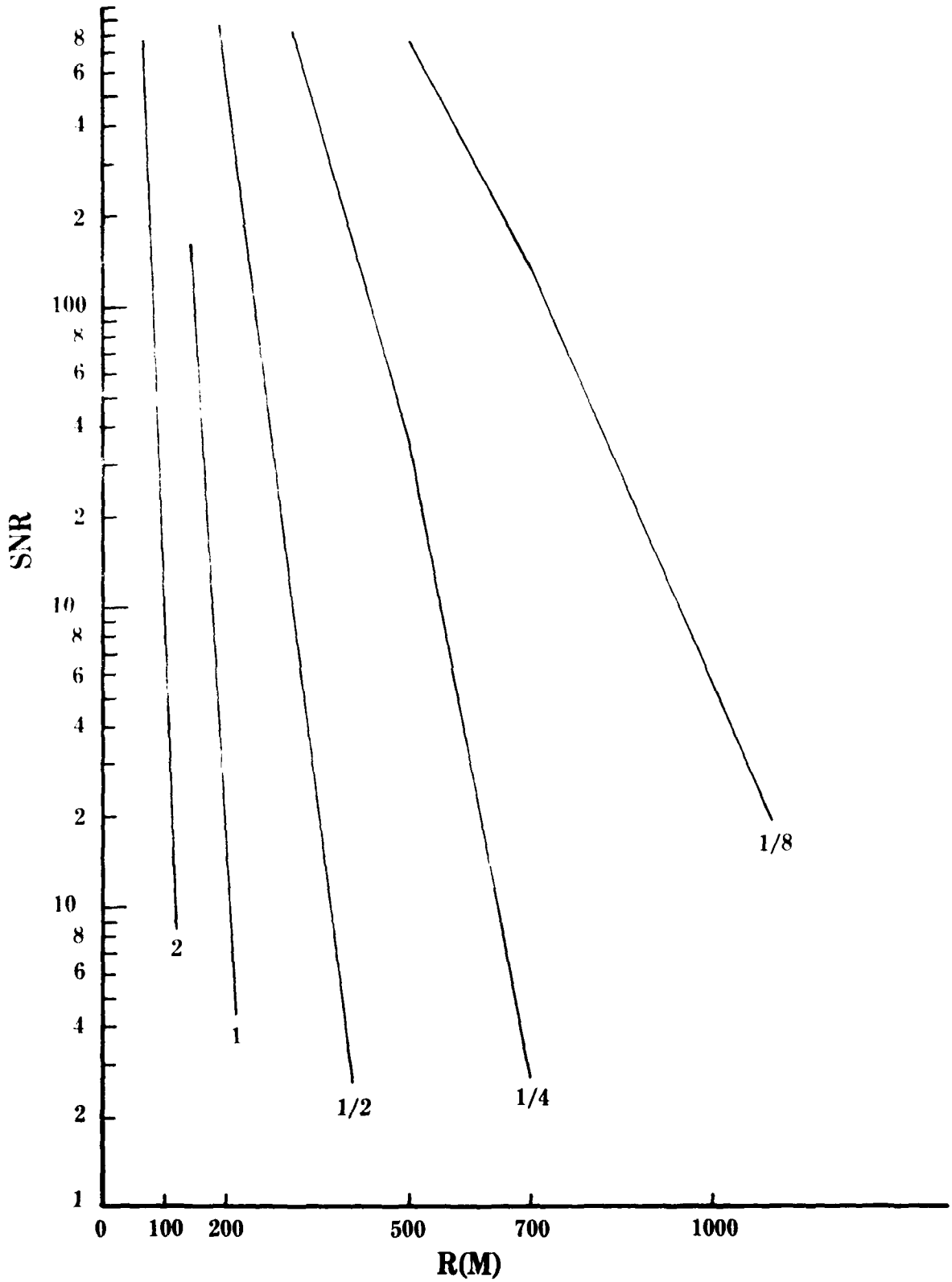

Figure 10. Signal-to-noise ratio as a function of depth (λ = 0.53μm, Distribution A).

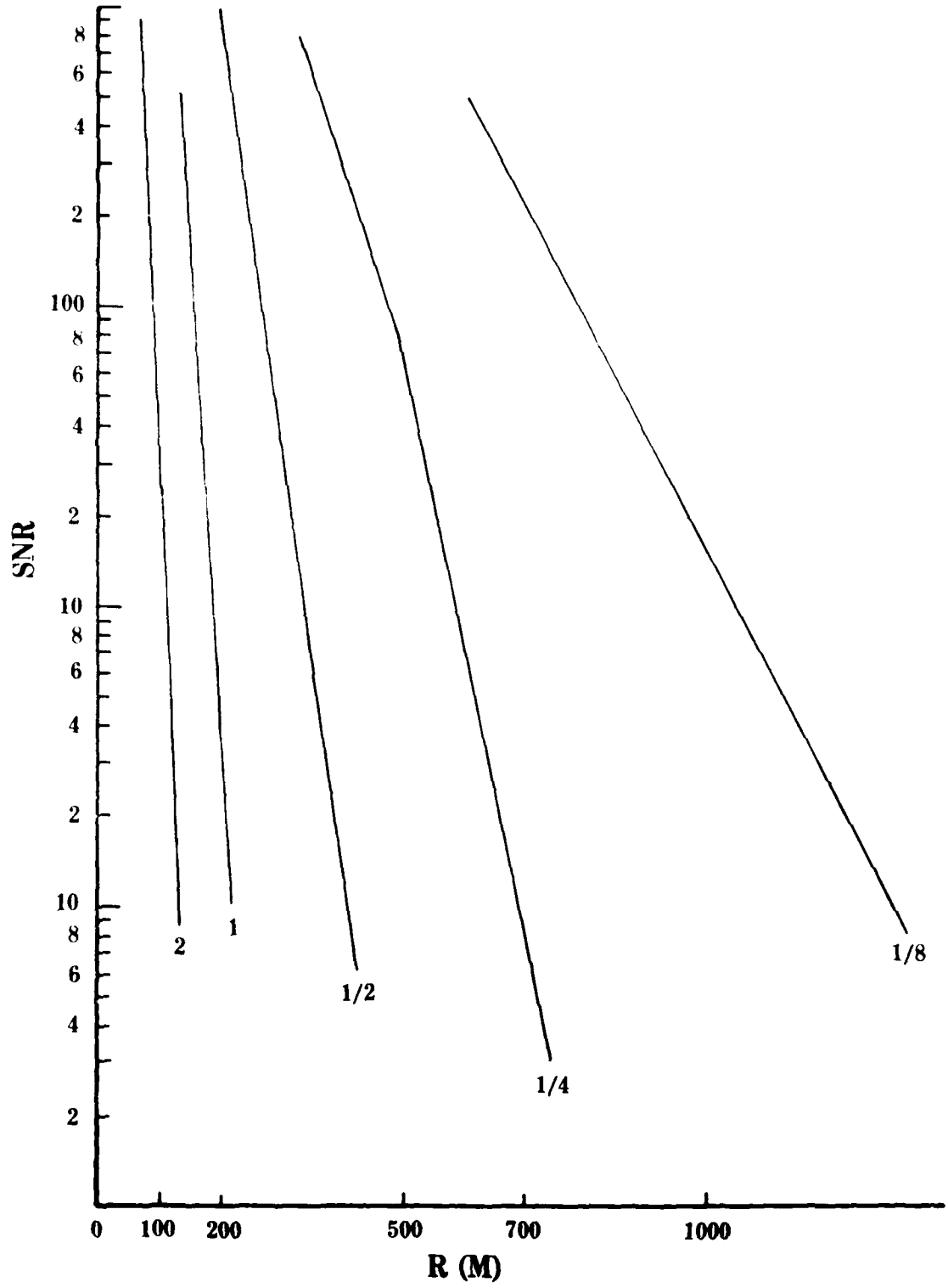

Figure 11. Same as in figure 10 (λ = 1.06μm).

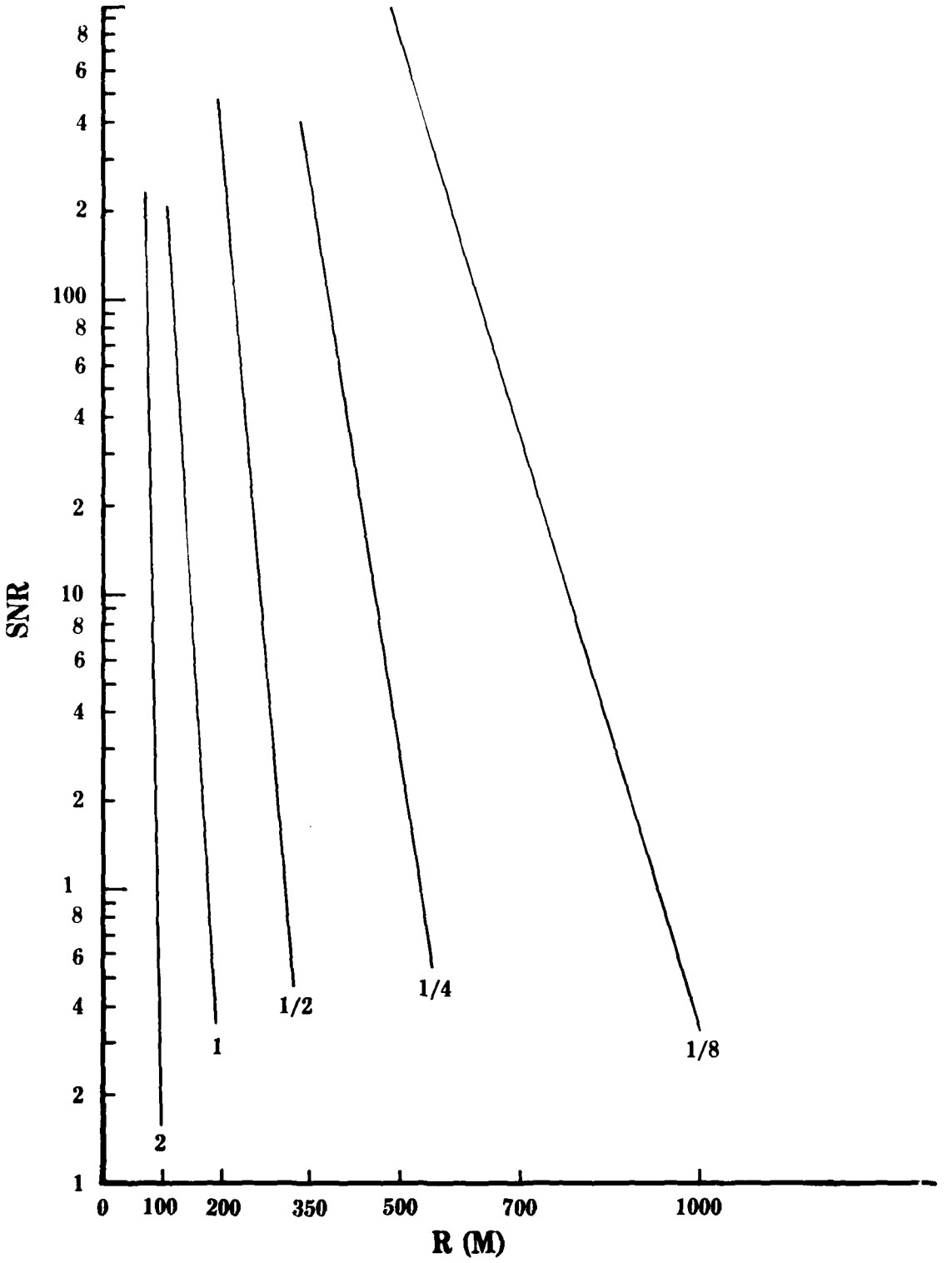

Figure 12. Same as in figure 10 (λ = 3.8μm).

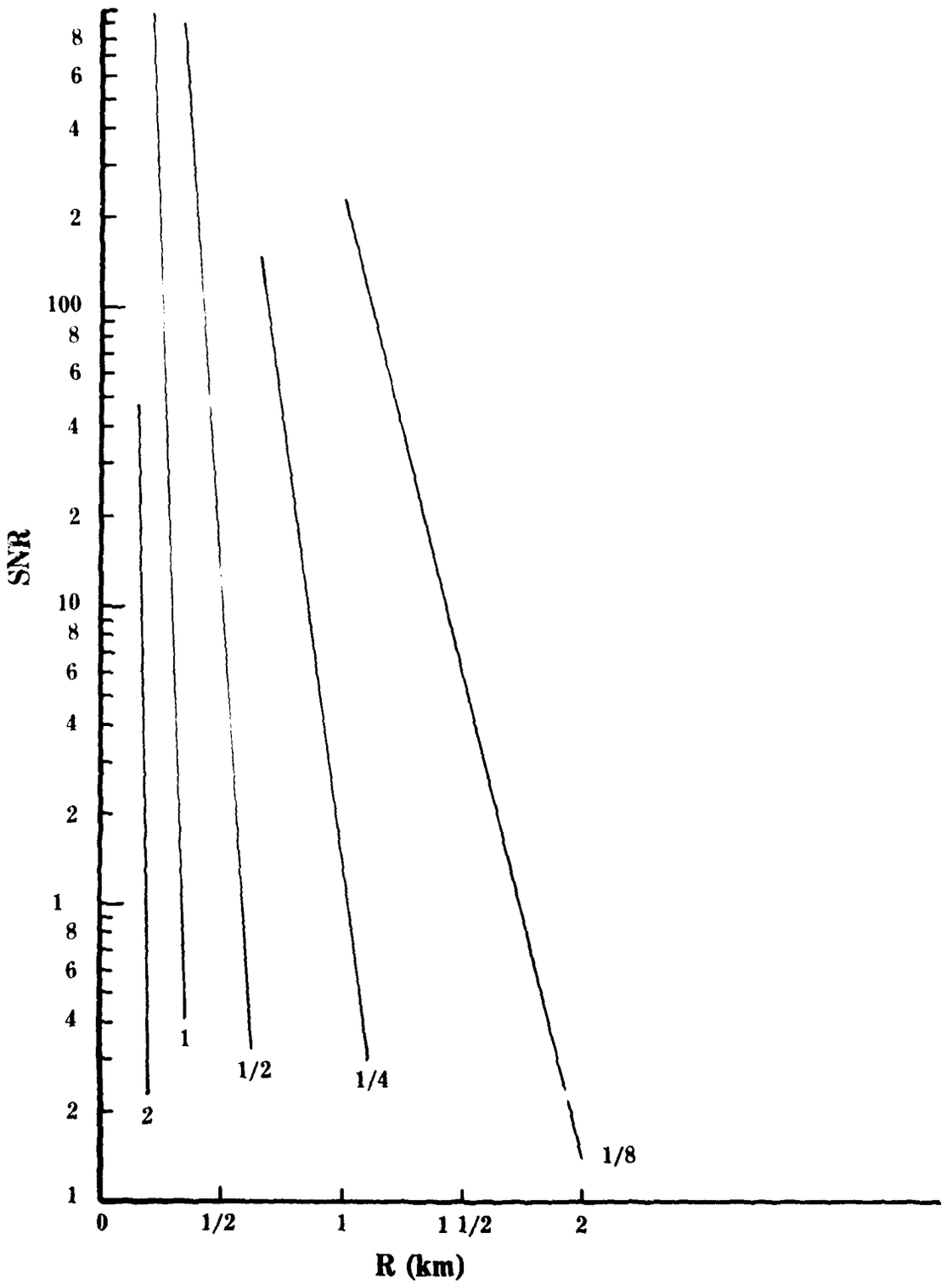

Figure 13. Same as in figure 10 (λ = 10.6μm).

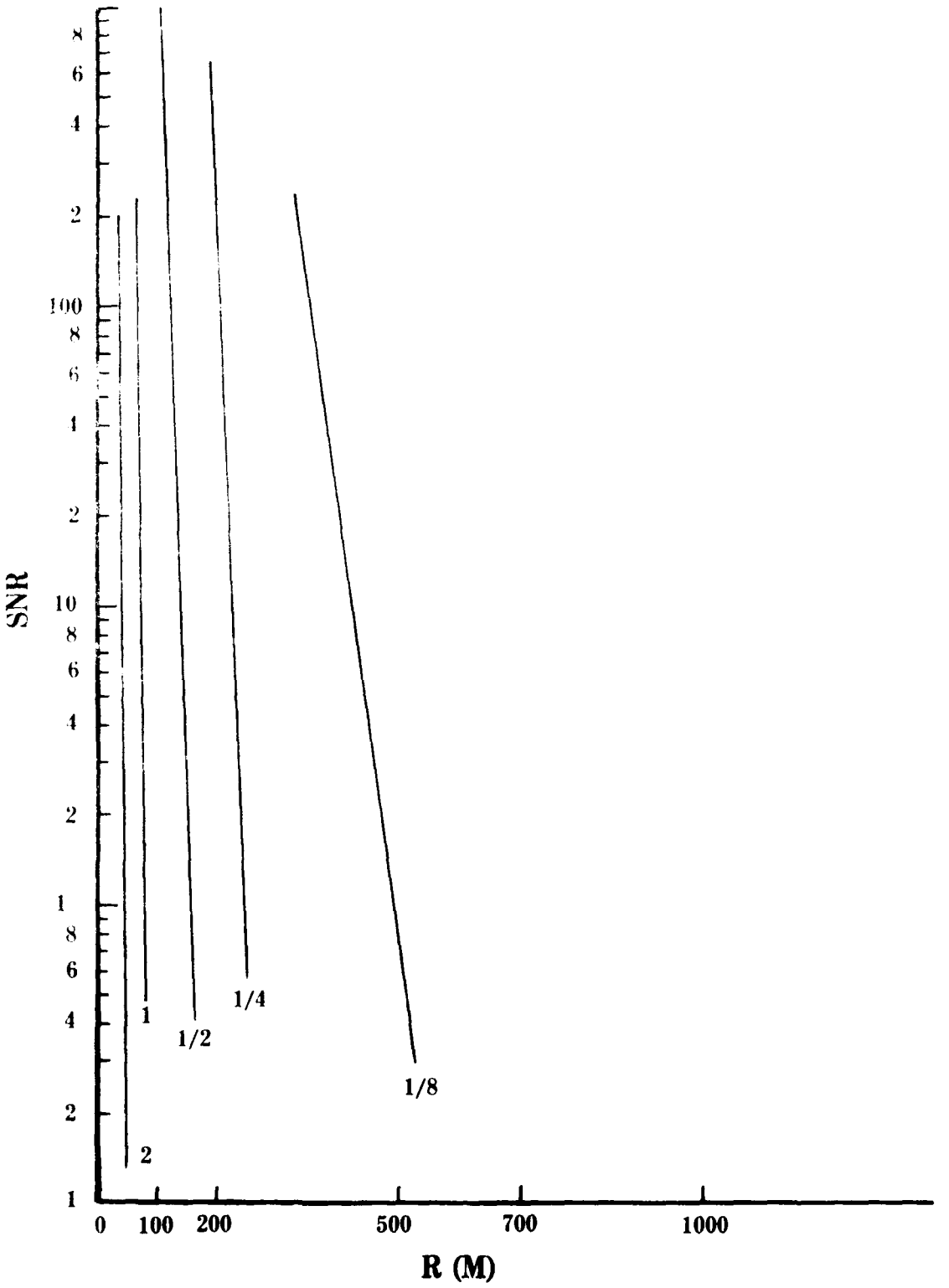

Figure 14. Signal-to-noise ratio as a function of depth (λ = 0.53μm, Distribution B).

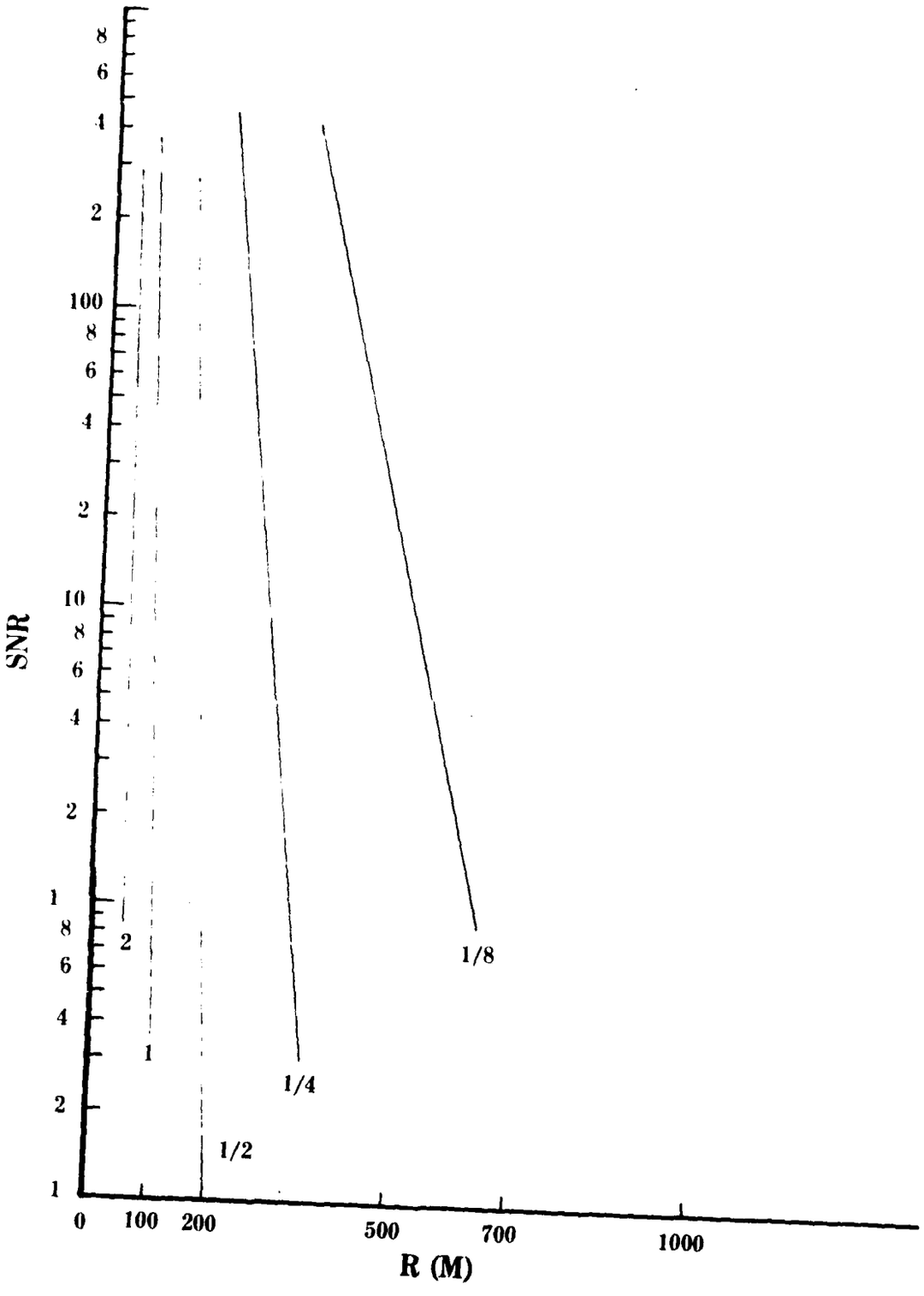

Figure 15. Same as in figure 14 (λ = 1.06μm).

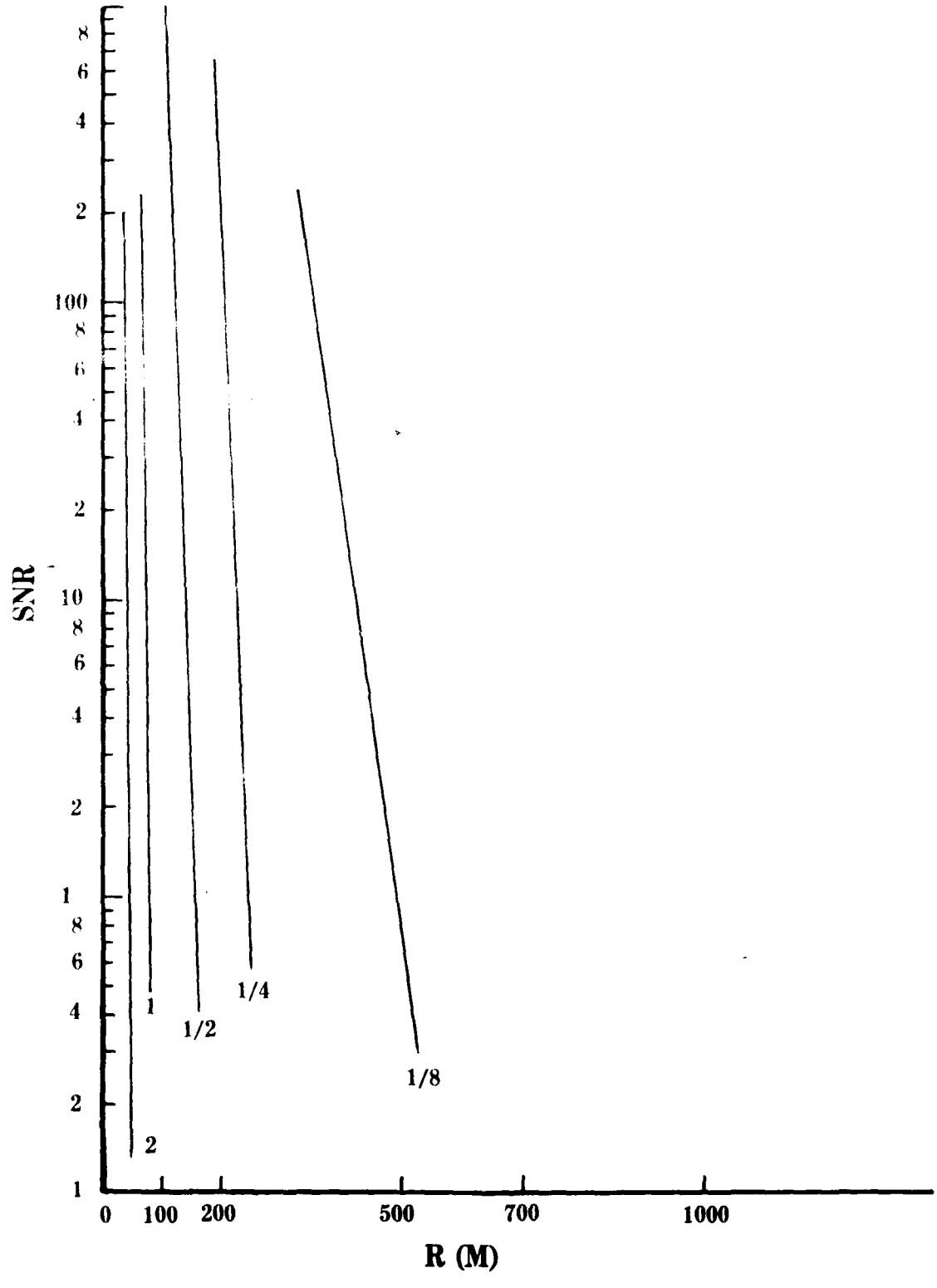

Figure 16. Same as in figure 14 (λ = 3.8μm).

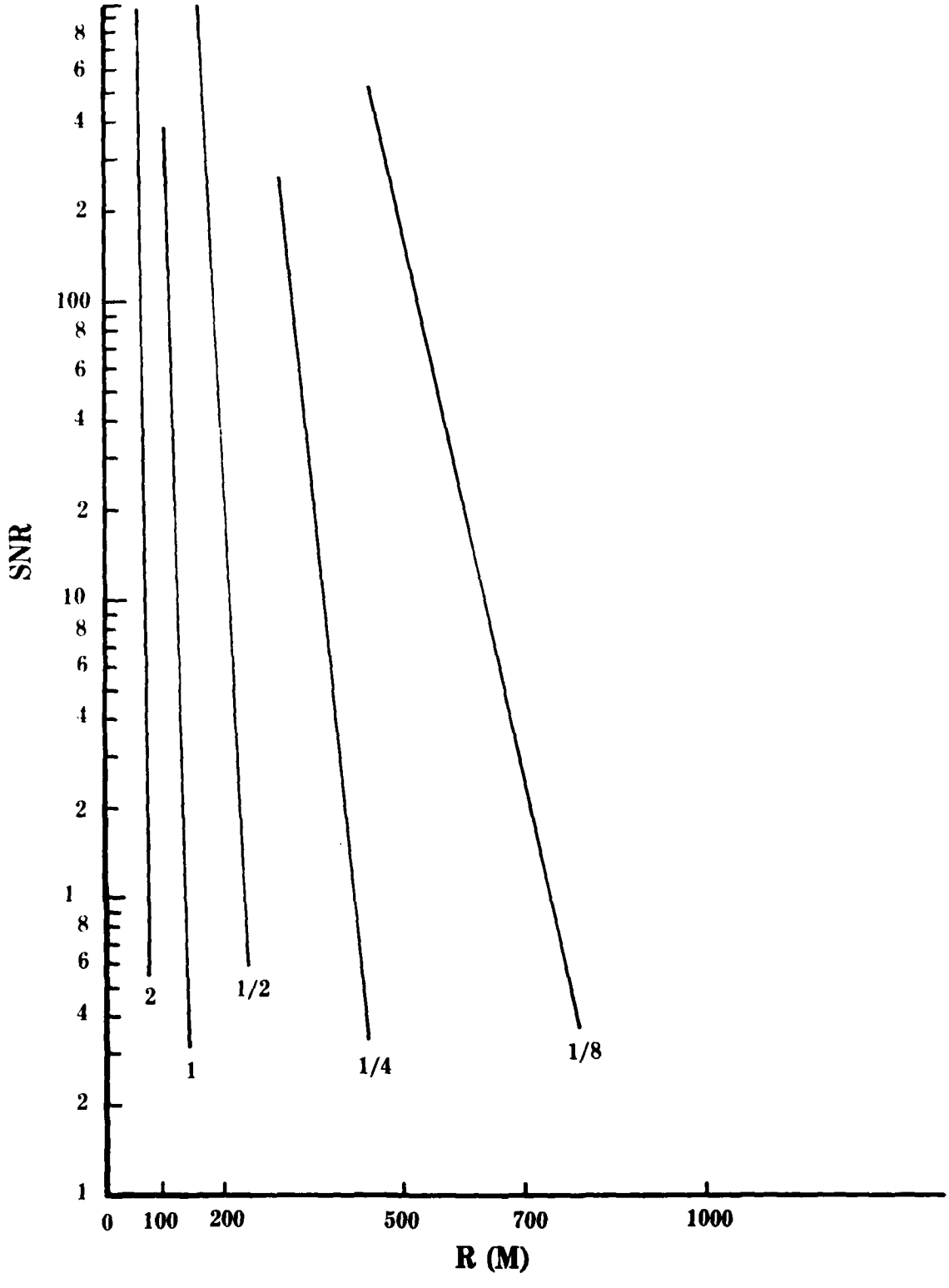

Figure 17. Same as in figure 14 (λ = 10.6μm)

$$P_r(R_1,t) = A \frac{cJ}{2R_1^2} \left[\overline{\beta(R_1)} + \beta'(R_1,t)\right] e^{-2} \int_0^{R_1} \left[\overline{Q_{TV}(R)} + Q'_{TV}(R,t)\right] dR \quad (4)$$

The time average $\overline{P_r(R_1,t)}$ will reduce the term containing $\beta'(R_1,t)$ to a negligible value under the assumption that the spatial average of the random variable $Q'(R,t)$ performed in the exponential integral is suitably small. Equation (4) then takes the form

$$\overline{P_r(R_N)} \simeq A \frac{cJ_\lambda}{2R_N^2} \left[\overline{\beta(R_N)}\right] e^{-2} \int_0^{R_N} \overline{Q_{TV}(R)}\, dR \,. \quad (5)$$

Writing it logarithmically yields

$$\overline{\ln P_r(R_n)} \simeq \ln C - 2 \ln R_n + \overline{\ln \beta(R_n)} - 2 \int_0^{R_n} \overline{Q_{TV}(R)}\, dR \,,$$

where $C = ACJ_\lambda/2$, and the averages are time averages of the returns, all from range R_n. We will drop the bars in the subsequent discussion. Now, if the value of $Q_{TV}(R)$ can be considered to be a mean over the distance from 0 to R_n, it can be taken out of the integral, making the last term $2\, Q_{TV}(R_n)\, R_n$, where $Q_{TV}(R_n)$ is the effective average volume extinction over the path from 0 to R_n.

Now, we assume we have returns from a large number of distances R_n, n = 1, 2, ..., N. We can then compute the effective averages for β and Q_{TV} from the entire set of returns in a least-squares sense in the following manner. We take the sum of all the returns for all R_n, n = 1, 2, ..., N. Thus

$$\sum_{n=1}^{N} \left[\ln P_R(R_n) = \ln C - 2 \ln R_n + \ln \beta(R_n) - 2\, Q_{TV}(R_n)\, R_n\right].$$

We now ask the question as to what is the best single value for β and Q_{TV} to fit all the measurements in a least-squares sense. Thus,

$$\sum_{n=1}^{N} \left[\ln P_R(R_n) - \ln C + 2 \ln R_n - \ln \beta + 2 Q_{TV} R_n \right]^2 = \Delta ,$$

where we want to minimize Δ. Therefore, take $\partial\Delta/\partial\beta$ and $\partial\Delta/\partial Q_{TV}$, and set each to zero, then solve the pair of equations for β and Q_{TV} to yield the best fit. This is straightforward and yields

$$\ln \beta = \frac{\sum_{n=1}^{N} \ln P_R(R_n) + 2 \sum_{n=1}^{N} \ln R_n + 2 Q_{TV} \sum_{n=1}^{N} R_n}{N} - \ln \frac{AC}{2}$$

$$Q_{TV} = \frac{\left[\sum_{n=1}^{N} R_n \sum_{n=1}^{N} \ln P_R(R_n) - N \sum_{n=1}^{N} \ln P_R(R_n) R_n \right] + 2 \left[\sum_{n=1}^{N} R_n \sum_{n=1}^{N} \ln R_n - N \sum_{n=1}^{N} R_n \ln R_n \right]}{2N \sum_{n=1}^{N} R_n^2 - 2 \sum_{n=1}^{N} R_n \sum_{n=1}^{N} R_n} .$$

These two expressions should yield values of $\ln \beta$ and Q_{TV} which fit the measurements of P_R at various ranges R_n, best in a least-squares sense. Note that they fit the logarithmic form of the lidar equation best.

Now, one could get "best-fit" values of β and Q_{TV} over different segments of the entire path. Thus, the entire path could be broken up into segments R_{N1}, R_{N2}, R_{N3}, ..., etc. Over each segment, say R_{N1}, a best fit for Q_{TV} and

I_{NB} could be obtained. The value for Q_{TV} could then be used to get the incident beam strength on the next segment, I_{N2}, and a similar procedure could be used to compute best-fit values over the next segment. This could be repeated as required.

b. Determination of Liquid Water Content

Figure 18 demonstrates more clearly the relationship of liquid water content to Q_{TV} of the fog. In this figure, the values of Q_{TV} for all of the modifications of distributions A and B are plotted for each of the four wavelengths. Noting that all of the calculations of Q_{TV} were for a fixed LWC of 1 gm/m^3, it is clear that, in order for a determination of Q_{TV} to be interpreted as a measure of the LWC of the fog, there must be a unique, or nearly unique, relationship of Q_{TV} to LWC. This relationship must be independent of the unknown size distribution. This figure shows that, at the two longer wavelengths, and particularly at the longest wavelength (10.6 μm), the relationship is indeed nearly unique. Thus, for the present set of calculations, all size distributions employed yielded a value of $Q_{TV} \approx .16\ m^{-1}$ for an LWC = 1.0 g/m^3. If the LWC were doubled, the resulting Q_{TV} would also be doubled. It is, of course, possible that real fogs may, in fact, have size distributions so grossly different from the wide range of possibilities considered here that this apparent relationship would break down. However, from the broad range of possibilities considered here, it does appear that a measure of Q_{TV} at 10.6 μm will provide a reasonable estimate of the LWC in the fog. These results are consistent with those of Pinnick *et al.* (1978b) and with the theoretical study of Chylek (1978).

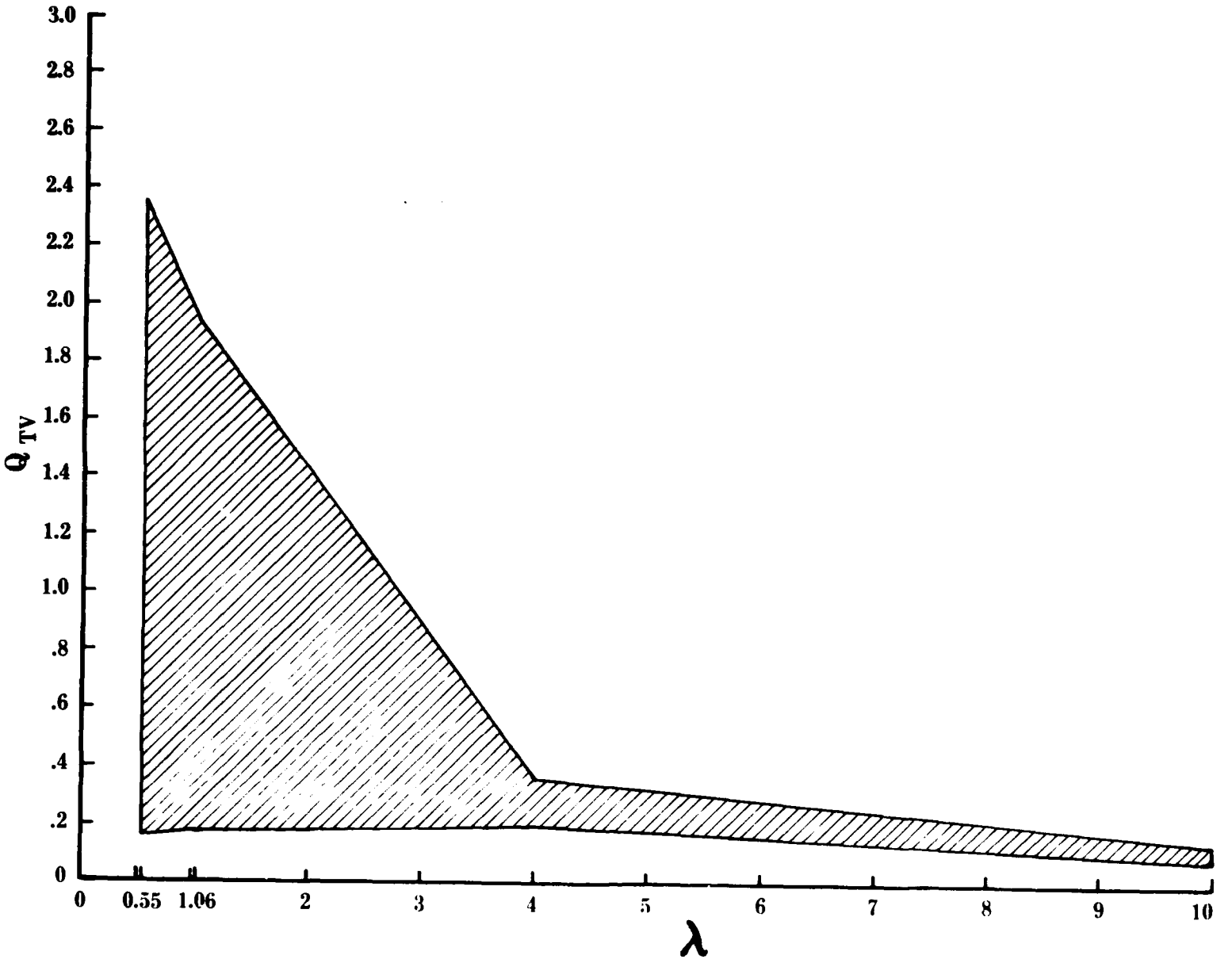

Figure 18. Volume extinction coefficient, Q_{TV}, plotted against λ for a fixed liquid water content.

6. Conclusions

The results of this study can be summarized by the following statements:

a. The penetration of the lidar pulse into the fog is limited to a few hundred meters due to the severe attenuation of the pulse by the fog. The penetration depth increases with increasing wavelength, as shown in Figures 10 through 17, in which the usefulness of the returned signal is measured by its signal-to-noise ratio.

b. Methods are suggested to obtain the averages of β and Q_{TV} which utilize both multiple-pulse temporal and least-squares spatial averaging procedures.

c. It has been shown, consistent with the literature, that liquid water content can be effectively measured from a knowledge of $\langle \overline{Q_{TV}} \rangle$ using a 10.6 μ lidar. Further, these studies indicate that lidar operating at a wavelength of 4 μ would also be useful for this purpose.

7. Recommendations for Future Work

a. It is recommended that experimental verification of the techniques for obtaining Q_{TV}, β, and LWC, as outlined in this report, be undertaken to determine the practical feasibility of our results. The required laser systems and components assumed in this study are currently available, and therefore such a program is now possible.

b. At optical depths exceeding a few tenths, which in most fogs is reached within tens of meters or less, multiple scatter effects may become important. It is recommended that theoretical and experimental studies of these effects be undertaken. The theoretical treatment of multiple scatter

of laser beams is quite complex, although some models have been developed. Nevertheless, this problem cannot be adequately studied in a short time period such as was available for the current work, and it is recommended that adequate financing and time be made available for a proper treatment of this problem.

c. The values of Q_{TV} and β at the four wavelengths used in this study contain some information as to the size distribution of the droplets composing the fog. A complete set of these parameters would represent 8 pieces of information, in the absence of errors of any type. The presence of errors (*e.g.*, measurement errors, numerical quadrature errors, etc.) will undoubtedly reduce the amount of independent data below the original 8 pieces. Nevertheless, it would appear that at least an estimate of the size distribution could be obtained through appropriate inversion techniques. It is recommended that this problem be studied to gain an insight as to how well the size distribution functions may be determined.

REFERENCES

Chylek, P., 1978: Extinction and liquid water content of fogs. *J. Atmos. Sci.*, **35**, 296-300.

Pinnick, R. G., D. L. Hoihjelle, G. Fernandez, E. B. Stenmark, J. D. Lindberg, S. G. Jennings, and G. B. Hoidale, 1978a: Vertical structure in atmospheric fog and haze and its effect on extinction. U. S. Army Electronics Research and Development Command, Atmospheric Sciences Laboratory, White Sands Missile Range, N. M., ASL-TR-0010, July.

Pinnick, R. G., S. G. Jennings, and P. Chylek, 1978b: Experimental verification of a linear relation between IR extinction and liquid water content of fogs. Third Conference on Atmospheric Radiation, June 28-30, 1978, Davis, Calif. Published by the American Meteorological Society, Boston, Mass.

Wolfe, W. L., and G. J. Zissis, 1978: *The Infrared Handbook*. Office of Naval Research, Department of the Navy, Arlington, Va., Chapter 4.

END

DATE
FILMED

8-80

DTIC